

Los Alamos

NATIONAL LABORATORY

memorandum

Los Alamos Neutron Science Center, LANSCE-1
Accelerator Physics and Engineering Group

To: Distribution
From: Barbara Blind, LANSCE-1, H808
Phone/Fax: 5-2607/5-2904
Symbol: LANSCE-1:99-065
Date: April 9, 1999
Email: bblind@lanl.gov

SUBJECT: Tracking of Partially Chopped Beams

Introduction

For the SNS project, the macropulse from the ion source must be transformed into a beam with the proper time structure for injection into a storage ring, namely 546-ns-long beam pulses with 295-ns-long gaps. This is accomplished in the MEBT, with a chopper that deflects the beam into an aperture referred to as the chopper stopper. In case of a sufficiently fast rise time of the chopper pulse, the micropulses experience no deflection for 546 ns and full deflection for 295 ns. These micropulses will be referred to as the unchopped beam and the fully chopped beam, respectively.

However, the chopper rise time is expected to be such that one or more micropulses will experience a partial deflection. Such micropulses are referred to as partially chopped beams. These partially chopped beams will not be entirely stopped by the chopper stopper. Therefore, the MEBT has an antichopper. The antichopper returns the partially chopped beams to the axis for proper transport through the remainder of the machine.

The notion has been promoted that a partially chopped beam will exit the CCL displaced in phase space from the unchopped beam in such a way that some of it will miss the injection foil of the ring. It is immediately obvious that this is possible if the chopper and antichopper pulses are not synchronized or the phase advance between chopper and antichopper is wrong.

This memo addresses the transport of partially chopped beams for perfectly synchronized chopper and antichopper pulses, and with the appropriate phase advance between chopper and antichopper.

The particle-tracking code PARMILA was used for the MEBT and DTL, and the particle-tracking code LINAC was used for the CCDTL and CCL. Particle tracking is usually done using a 2D space-charge routine and neglecting image charges. In this case, no evidence was found that the partially chopped beams exit the CCL outside the phase space of the unchopped beam. When taking into account image charges in the MEBT and DTL, this result remains unchanged. When using the more precise 3D space-charge routine in PARMILA, the beams develop more halo than when using the usual 2D space-charge

routine. However, the partially chopped beams at the exit of the CCL are again inside the phase space of the unchopped beam.

Overview of Computations

This memo first presents the results from two initial sets of runs to simulate the chopping process. One set of runs was for a machine (defined as MEBT, DTL, CCDTL and CCL) without errors, the other set of runs was for a machine with errors. Each set of runs consisted of four cases, representing chopper deflections such that approximately 100%, 75%, 50% and 25% of the beam remains downstream of the chopper stopper. For the four cases, the beam was deflected by the chopper and antichopper by 0.0 mrad, 6.7 mrad, 8.9 mrad, and 11.0 mrad, respectively.

The code PARMILA was used to transport the beam through the MEBT and DTL, and the code LINAC was used to transport the beam through the CCDTL and CCL. PARMILA was executed with its default settings. Thus, image charges were not included in the PARMILA computations. For LINAC, image charges are not an option. In both PARMILA and LINAC, the usual 2D space-charge routine was used.

Phase-space plots of the unchopped and partially chopped beams at the exit of the CCL are presented in the memo. For both sets of runs, the partially chopped beams are within the phase space of the unchopped beam, at the exit of the CCL as well as at the exit of the MEBT and at the exit of the DTL.

Image charges were identified as a mechanism for steering each partially chopped beam differently from the unchopped beam. In PARMILA, the option existed for considering image charges in the drift tubes of the DTL. Phase-space plots of sample DTL output beams from particle tracking with and without image charges in the drift tubes are shown in the memo. Later, the option of image charges in the drifts and quadrupoles was added to PARMILA by Bob Garnett, and the runs were repeated assuming image charges in the MEBT and DTL. Again, phase-space plots of sample DTL output beams are presented. At the exit of the DTL, there is no evidence of beam steering due to the image charges. Image charges were not implemented in LINAC.

The issue also came up whether the 3D space-charge routine written by Frank Guy would yield significantly different results from the usually used 2D space-charge routine written by Ken Crandall, especially for the partially chopped beams. The 3D space-charge routine was installed in PARMILA by George Neuschaefer. The 3D space-charge routine was not installed in LINAC. The two sets of runs were repeated using the 3D space-charge routine in the MEBT and DTL. The memo shows phase-space plots of the unchopped and partially chopped beams at the exit of the DTL for the set of runs without machine errors, for beams transported with the 2D as well as the 3D space-charge routine. The phase-space distributions at the exit of the DTL are reasonably similar for the two space-

charge routines. For both sets of runs, the partially chopped beams at the exit of the DTL are inside the phase space of the unchopped beam.

All the DTL output beams obtained from tracking with the 3D space-charge routine were transported to the exit of the CCL using LINAC with the 2D space-charge routine. Phase-space plots of the unchopped and partially chopped beams at the exit of the CCL are presented in the memo, for the machine without and the machine with errors. The beams of these final sets of runs have somewhat more halo than the beams of the initial sets of runs. However, for both sets of runs the partially chopped beams are again inside the phase space of the unchopped beam.

In all runs, the same 9269-particle distribution was used as MEBT input beam. This was an output beam of an RFQ with a particular set of errors. The machine contained the modified baseline MEBT discussed in an earlier memo [1].

No Image Charges, 2D Space-Charge Routine

There were two sets of runs, one where the beam was tracked through a MEBT, DTL, CCDTL and CCL without errors, and one where it was tracked through a MEBT, DTL, CCDTL and CCL with errors. For the set of runs with machine errors, the error limits in the MEBT, DTL, CCDTL and CCL were as detailed in the earlier memo [1]. There were 2.0-mil limits on the transverse misalignments of the MEBT quadrupoles. Identical errors were present in all runs.

For each set of runs, the beam was steered by 0.0 mrad, 6.7 mrad, 8.9 mrad, and 11.0 mrad, respectively, by the chopper and antichopper. The aperture representing the chopper stopper removed a fraction of each beam. The beam was not artificially brought back to the axis at the exit of the MEBT and the steering in the CCDTL and CCL was turned off. With the steering turned on, the partially chopped beams would be steered differently from the unchopped beam. Since the steering remains constant during chopping, this would be the wrong description of the actual situation.

For the initial two sets of runs, the 2D space-charge routine was used and image charges were not considered.

For the set of runs without machine errors, the number of particles downstream of the chopper stopper was 9258, 6953, 4574 and 2353, respectively, or about 99.9%, 75.0%, 49.3% and 25.4% of the input beam. For the set of runs with machine errors, the number of particles downstream of the chopper stopper was 9254, 6649, 4216 and 2031, respectively, or about 99.8%, 71.7%, 45.5% and 21.9% of the input beam. The numbers of particles remaining from the 9269-particle MEBT input beam are also shown as case 1 and case 2 of Table 1.

The xx' , yy' , and xy phase-space plots of the unchopped beam and the three partially chopped beams are shown in Figures 1a, 1b, and 1c, respectively, for the case without

Table 1. Number of particles remaining from 9269-particle MEBT input beam, for each chopper deflection and each case, as indicated.

deflection (mrad)	case 1	case 2	case 3	case 4	case 5
0.0	9258	9254	9254	9259	9257
6.7	6953	6649	6649	6908	6590
8.9	4574	4216	4213	4577	4224
11.0	2353	2031	2026	2366	2069

case 1: without machine errors, without image charges, 2D space-charge routine

case 2: with machine errors, without image charges, 2D space-charge routine

case 3: with machine errors, with image charges, 2D space-charge routine

case 4: without machine errors, without image charges, 3D space-charge routine

case 5: with machine errors, without image charges, 3D space-charge routine

machine errors, and in Figures 2a, 2b, and 2c, respectively, for the case with machine errors. In these plots, the dots belong to the 0.0-mrad deflections, the triangles to the 6.7-mrad deflections, the squares to the 8.9-mrad deflections and the diamonds to the 11.0-mrad deflections of the chopper and antichopper.

Clearly, the partially chopped beams are within the phase space of the unchopped beam. For the set of runs with machine errors, the partially chopped beams are more nearly centered on the unchopped beam than for the set of runs without machine errors. Because steering was turned off, the beams do not exit the CCL on axis for the case with machine errors.

Image Charges, 2D Space-Charge Routine

It was suggested that image charges might account for different steering of the partially chopped beams from the unchopped beam.

It was rediscovered that the effect of image charges in the drift tubes of a DTL could be simulated with PARMILA [2].

Thus, for the two sets of runs, the beams from a MEBT without image charges were sent through the DTL with image charges and compared to the DTL output beams without image charges.

At the exit of the DTL, there are rather insignificant differences between the particle coordinates of beams that were tracked with and without image charges in the drift tubes. The effect actually was largest for the unchopped beam and the machine with errors. For this case, the xx' , yy' , and xy phase-space plots are shown in Figures 3a, 3b, and 3c, respectively. The dots represent the beam that was tracked without image charges in the drift tubes and the triangles represent the beam that was tracked with image charges in the drift tubes.

Subsequently, Bob Garnett modified PARMILA, adding the image-charge calculation to the drifts and quadrupoles. Thus, it is now possible to simulate transport lines with image charges.

Consequently, the beams were tracked through the MEBT and DTL with image charges and with machine errors and compared to the DTL output beams without image charges and with machine errors. Even though the image charges have a very minor effect on the beam, there were now 9254, 6649, 4213 and 2026 particles, respectively, remaining from the 9269-particle input beam (see Table 1, case 3). The effect of the image charges is again shown for the unchopped beam. The xx' , yy' , and xy phase-space plots are shown in Figures 4a, 4b, and 4c, respectively. The dots represent the beam that was tracked without image charges in the MEBT and DTL and the triangles represent the beam that was tracked with image charges in the MEBT and DTL. The effects were similar for the partially chopped beams.

One might convincingly argue that since at the end of the DTL the effects of the image charges are small they will also be small at the end of the CCL. The beam still has to be accelerated from 20 MeV to 1 GeV, but it is becoming more rigid, it is in a larger-aperture pipe and its centroid is not going any further off axis than it has in the MEBT and DTL.

No Image Charges, 3D Space-Charge Routine

The usual space-charge routine is a 2D space-charge routine written by Ken Crandall. The mesh is an r-z mesh that is centered on the beam centroid. From experience, this space-charge routine is valid for beams of elliptical cross section, with aspect ratios of at least 3, and probably with aspect ratios of as high as 5 [3].

Other space-charge routines are also available. One of them is a 3D point-to-point space-charge routine written by Frank Guy [3]. The 3D space-charge routine was used to check that the tracking results are not significantly different from those obtained with the 2D space-charge routine.

George Neuschaefer installed the 3D space-charge routine in PARMILA. The beams were then transported through the MEBT and DTL using this routine. For chopper deflections of 0.0 mrad, 6.7 mrad, 8.9 mrad, and 11.0 mrad, 9259, 6908, 4577, and 2366 particles, respectively, remained downstream of the chopper stopper for the set of runs without machine errors, and 9257, 6590, 4224, and 2069 particles, respectively, remained for the set of runs with machine errors. These numbers are also shown as case 4 and case 5 of Table 1.

At the exit of the DTL, the beam when tracked with the usual 2D space-charge routine versus the more accurate 3D space-charge routine lies in similar phase spaces. In particular, the beams are not steered differently. There are some differences, though.

Figures 5a, 5b, and 5c, respectively, give the xx' , yy' , and xy phase-space plots for the unchopped beam (0.0-mrad deflections). Figures 6a, 6b, and 6c give the same for the 6.7-mrad deflections, and Figures 7a, 7b, and 7c give the same for the 8.9-mrad deflections. Finally, Figures 8a, 8b, and 8c give the same for the 11.0-mrad deflections. The dots belong to the beam tracked using the 2D space-charge routine, and the triangles belong to the beam tracked using the 3D space-charge routine.

For all beams, the linear focus appears to be slightly different for the 3D space-charge routine, relative to the 2D space-charge routine. In other words, the DTL output beams have different Twiss parameters when using the 2D versus the 3D space-charge routine. The beam parameters at the exit of the DTL are given in Tables 2 through 5. Table 2 represents the set of runs without machine errors and using the 3D space-charge routine. Table 3 represents the set of runs with machine errors and using the 3D space-charge routine. Table 4 represents the set of runs without machine errors and using the 2D space-charge routine. Finally, Table 5 represents the set of runs with machine errors and using the 2D space-charge routine.

Table 2. Parameters of DTL output beam for indicated deflections of chopper and antichopper, in units of mrad. No machine errors, 3D space-charge routine. Transverse units are mm and mrad, longitudinal units are $^\circ$ and keV.

deflection	α_x	β_x	ϵ_x	α_y	β_y	ϵ_y	α_ϕ	β_ϕ	ϵ_ϕ
0.0	4.191	1.770	0.241	-2.531	0.958	0.251	-0.091	0.111	158.1
6.7	3.451	1.419	0.220	-1.992	0.774	0.229	-0.098	0.109	147.9
8.9	2.909	1.271	0.206	-1.828	0.667	0.194	-0.189	0.080	157.2
11.0	2.748	1.202	0.214	-2.009	0.698	0.165	0.243	0.098	160.2

Table 3. Parameters of DTL output beam for indicated deflections of chopper and antichopper, in units of mrad. With machine errors, 3D space-charge routine. Transverse units are mm and mrad, longitudinal units are $^\circ$ and keV.

deflection	α_x	β_x	ϵ_x	α_y	β_y	ϵ_y	α_ϕ	β_ϕ	ϵ_ϕ
0.0	4.012	1.705	0.245	-2.423	0.915	0.279	-0.045	0.109	166.5
6.7	3.156	1.333	0.222	-1.834	0.717	0.244	-0.108	0.104	157.4
8.9	2.945	1.321	0.208	-1.957	0.695	0.196	-0.089	0.073	159.1
11.0	2.964	1.236	0.227	-1.716	0.616	0.163	-0.069	0.105	163.0

Table 4. Parameters of DTL output beam for indicated deflections of chopper. And antichopper. No machine errors, 2D space-charge routine. Transverse units are mm and mrad, longitudinal units are $^\circ$ and keV.

deflection	α_x	β_x	ϵ_x	α_y	β_y	ϵ_y	α_ϕ	β_ϕ	ϵ_ϕ
0.0	3.391	1.491	0.228	-2.267	0.807	0.239	-0.038	0.116	153.2
6.7	2.712	1.248	0.218	-2.244	0.749	0.225	-0.136	0.097	157.9
8.9	3.693	1.641	0.211	-2.580	0.862	0.222	0.107	0.068	169.6
11.0	3.359	1.335	0.203	-1.884	0.732	0.201	-0.124	0.112	192.3

Table 5. Parameters of DTL output beam for indicated deflections of chopper.
 And antichopper. With machine errors, 2D space-charge routine.
 Transverse units are mm and mrad, longitudinal units are ° and keV.

deflection	α_x	β_x	ϵ_x	α_y	β_y	ϵ_y	α_ϕ	β_ϕ	ϵ_ϕ
0.0	3.220	1.438	0.237	-2.284	0.798	0.267	-0.005	0.109	167.7
6.7	2.633	1.258	0.231	-2.274	0.755	0.232	-0.118	0.087	168.9
8.9	3.874	1.696	0.216	-2.729	0.907	0.230	0.254	0.074	170.2
11.0	3.491	1.358	0.219	-1.588	0.639	0.187	-0.494	0.102	200.1

The DTL output beams were transported through the CCDTL and CCL using LINAC with the 2D space-charge routine. For one final set of runs, this was done for a machine without errors, for the other final set of runs, it was done for a machine with errors.

The xx' , yy' , and xy phase-space plots of the unchopped and the three partially chopped CCL output beams are shown in Figures 9a, 9b, and 9c, respectively, for the case without machine errors, and in Figures 10a, 10b, and 10c, respectively, for the case with machine errors. Again, the dots belong to the 0.0-mrad deflections, the triangles to the 6.7-mrad deflections, the squares to the 8.9-mrad deflections, and the diamonds to the 11.0-mrad deflections of the chopper and antichopper.

Figures 9a, 9b, and 9c should be compared to Figures 1a, 1b, and 1c. Figures 10a, 10b, and 10c should be compared to Figures 2a, 2b, and 2c. The beams have more halo when the 3D space-charge routine is used than when the 2D space-charge routine is used. However, for the initial sets of runs as well as for the final sets of runs the partially chopped beams are inside the unchopped beam. For the sets of runs with machine errors, the partially chopped beams are more nearly centered on the unchopped beam than for the sets of runs without machine errors.

References

- [1] Barbara Blind and Robert Garnett, "SNS Baseline MEBT and Modified Baseline MEBT", LANSCE-1:99-061, April 5, 1999.
- [2] K. R. Crandall, "Image Charges", AT-1:88-340, October 5, 1988.
- [3] George Neuschaefer, private communication.

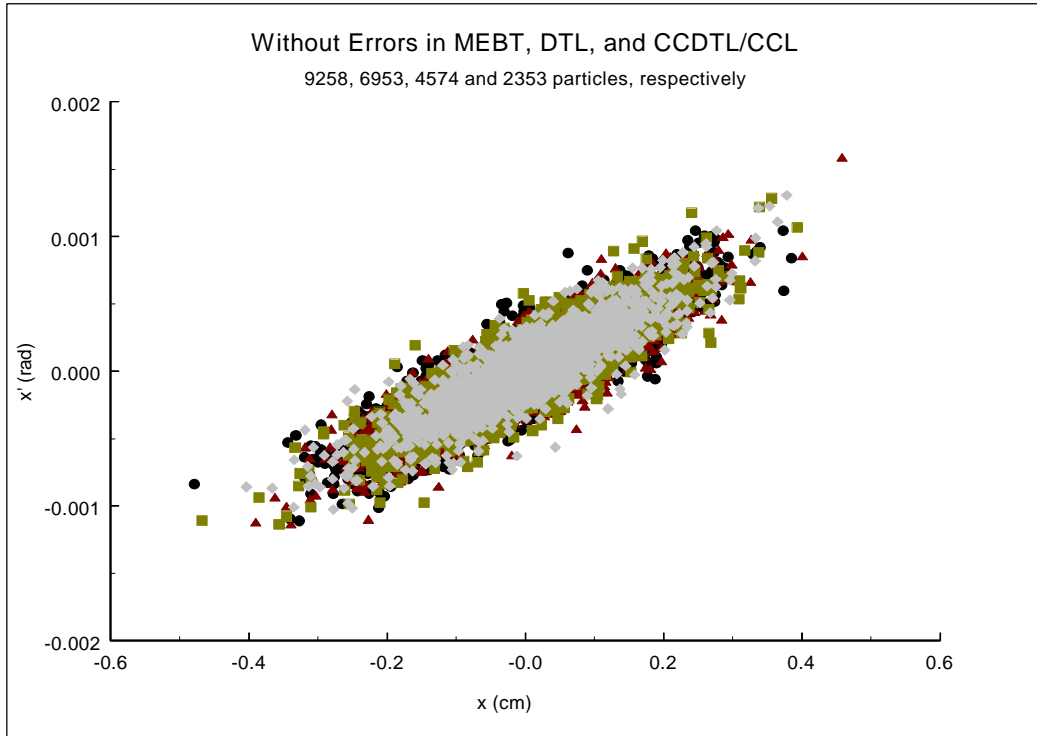


Figure 1a. Horizontal phase space of unchopped and partially chopped CCL output beams, no machine errors, no image charges, 2D space-charge routine.

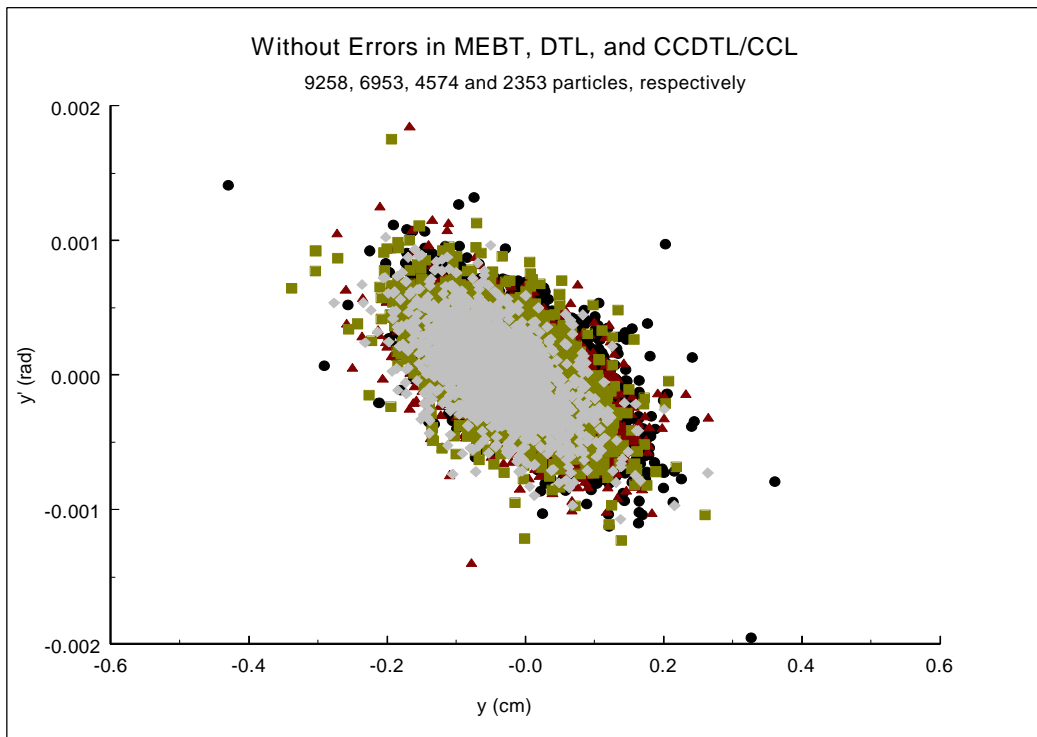


Figure 1b. Vertical phase space of unchopped and partially chopped CCL output beams, no machine errors, no image charges, 2D space-charge routine.

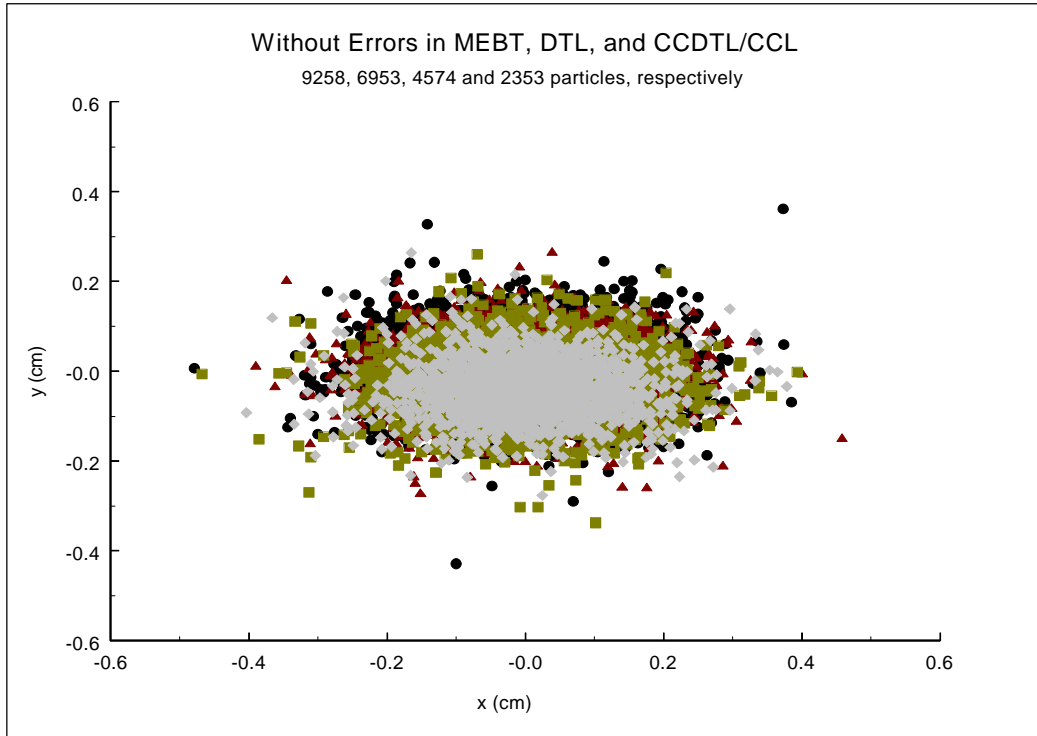


Figure 1c. Footprints of unchopped and partially chopped CCL output beams, no machine errors, no image charges, 2D space-charge routine.

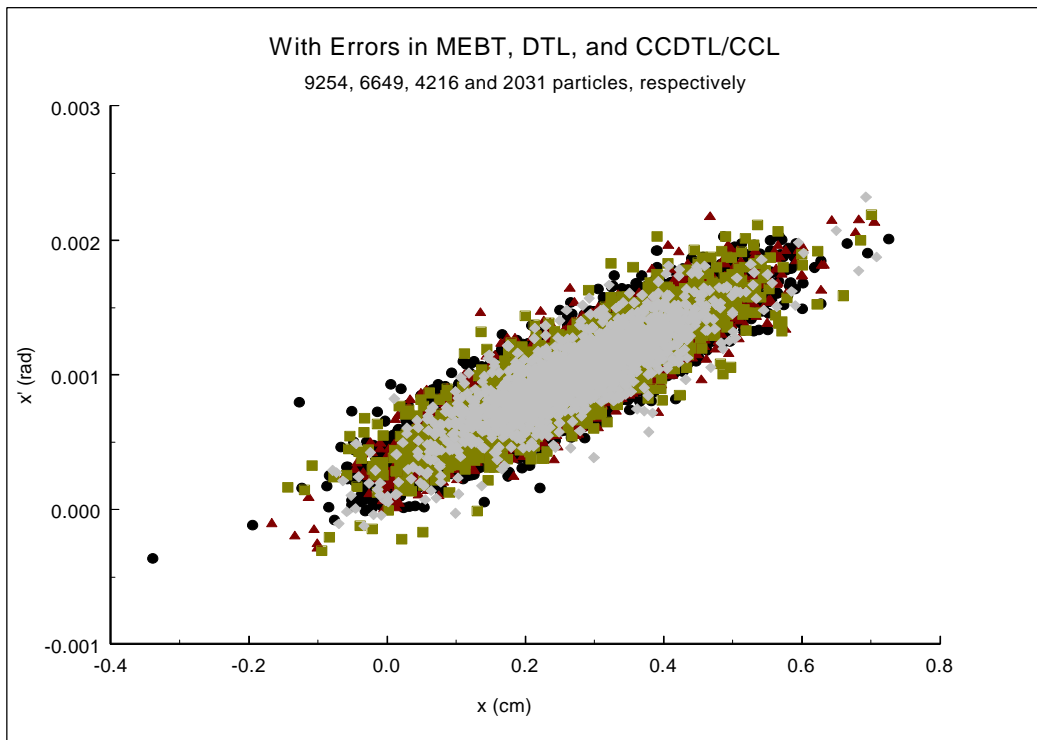


Figure 2a. Horizontal phase space of unchopped and partially chopped CCL output beams, machine errors, no image charges, 2D space-charge routine.

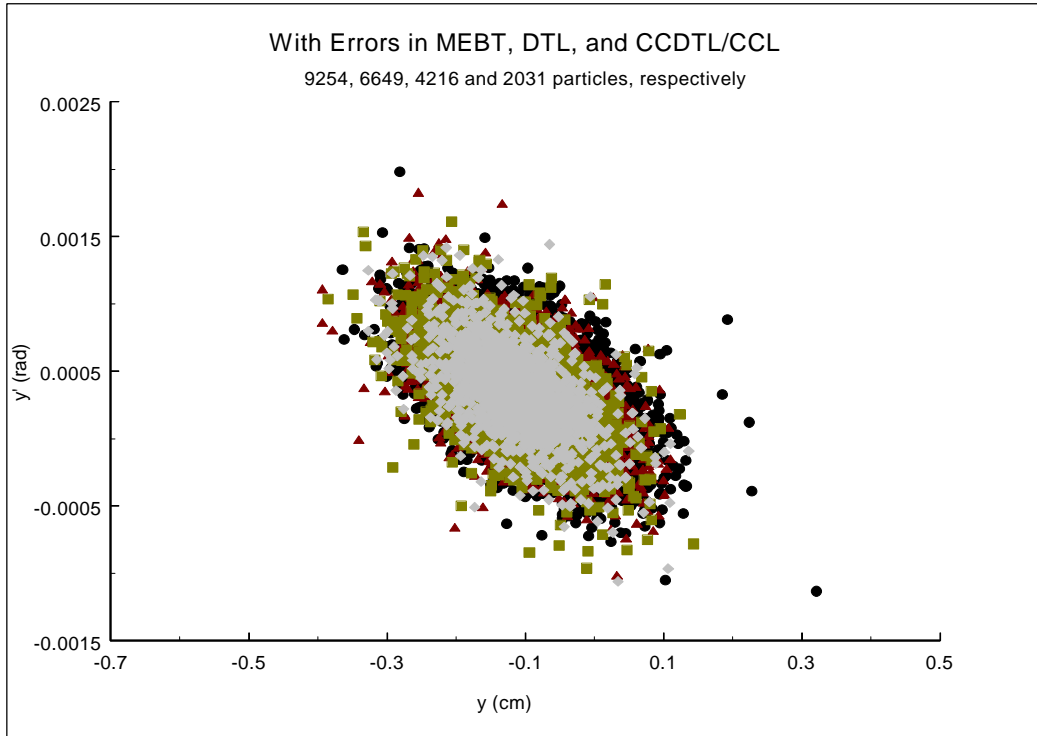


Figure 2b. Vertical phase space of unchopped and partially chopped CCL output beams, machine errors, no image charges, 2D space-charge routine.

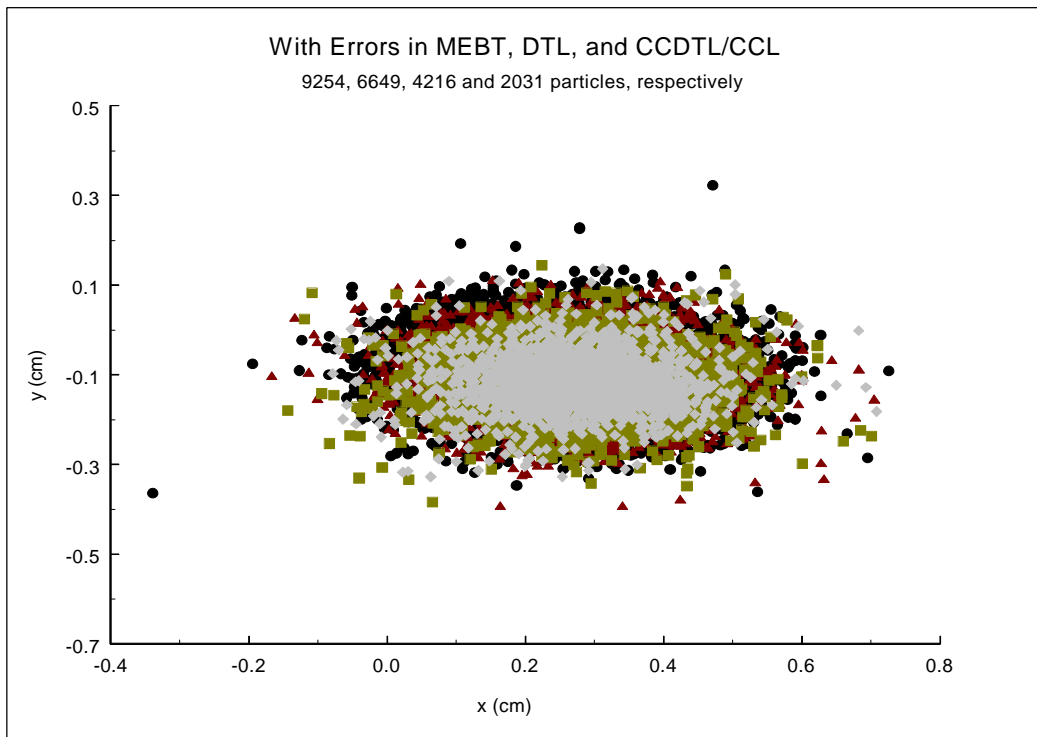


Figure 2c. Footprints of unchopped and partially chopped CCL output beams, machine errors, no image charges, 2D space-charge routine.

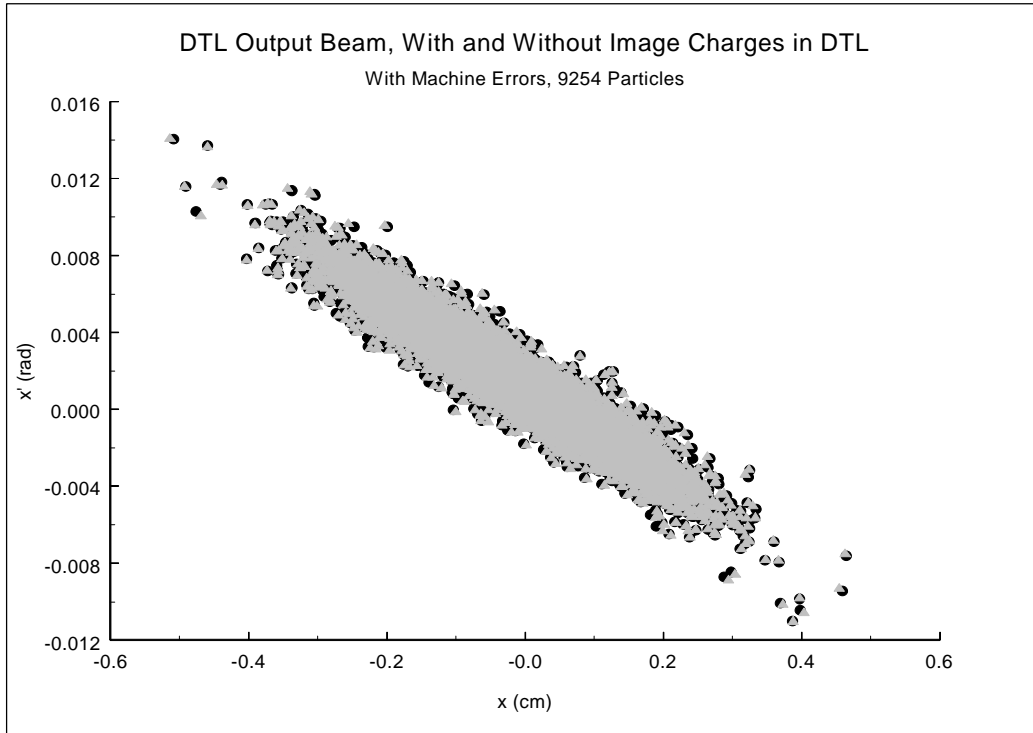


Figure 3a. Horizontal phase space of unchopped DTL output beam, machine errors, 2D space-charge routine, with and without image charges in DTL.

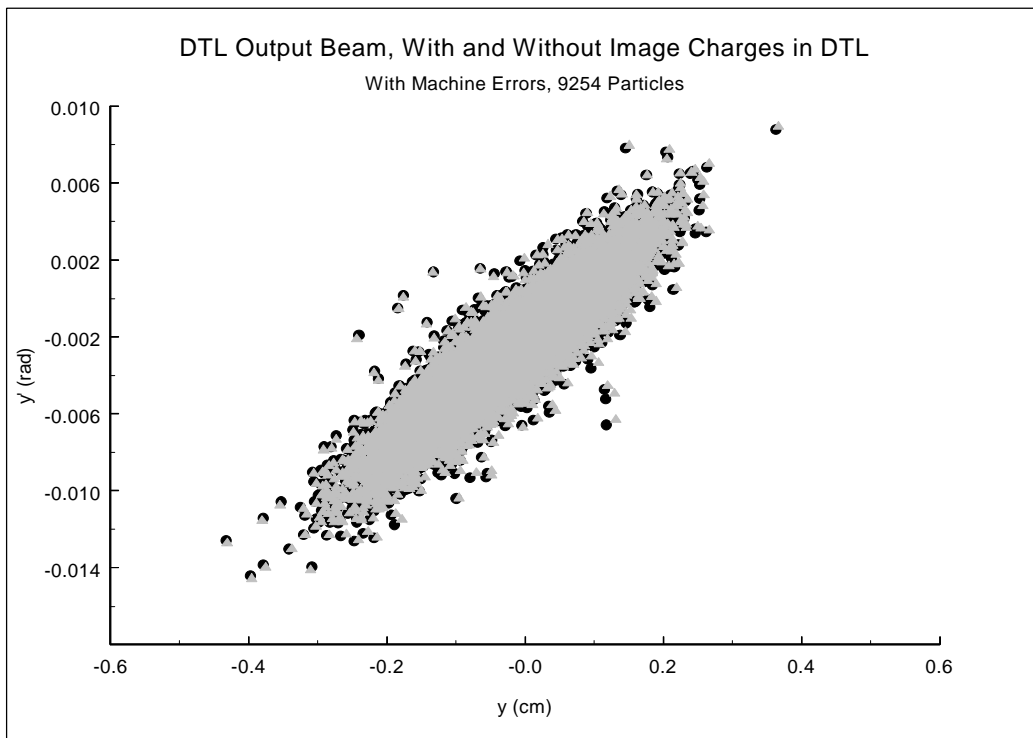


Figure 3b. Vertical phase space of unchopped DTL output beam, machine errors, 2D space-charge routine, with and without image charges in DTL.

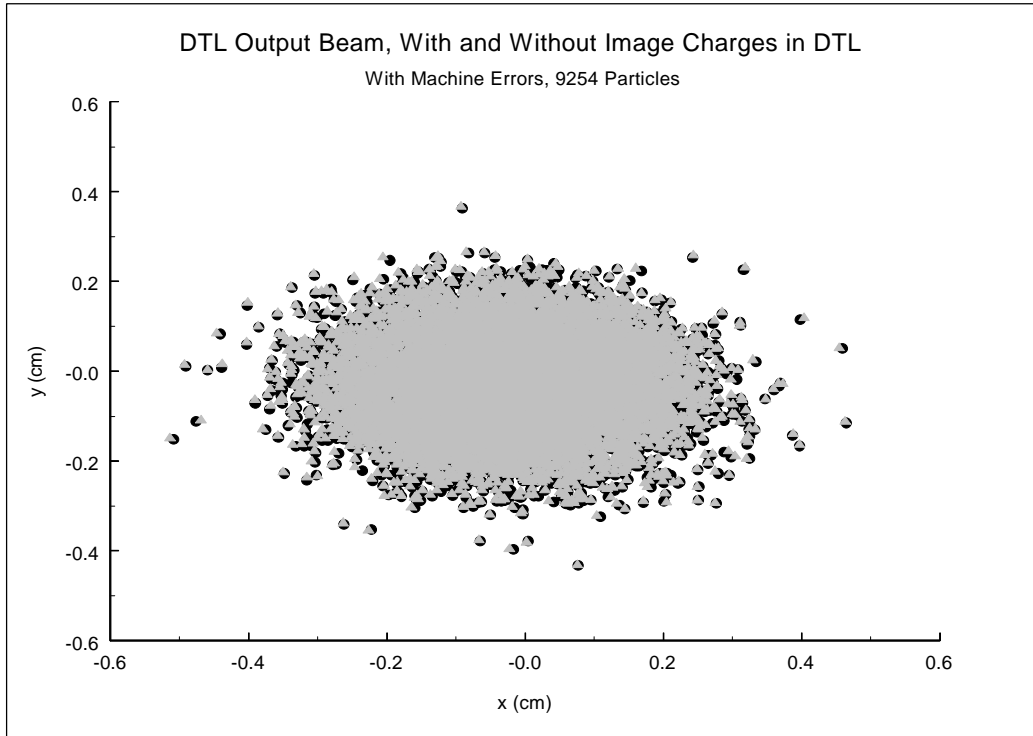


Figure 3c. Footprints of unchopped DTL output beam, machine errors, 2D space-charge routine, with and without image charges in DTL.

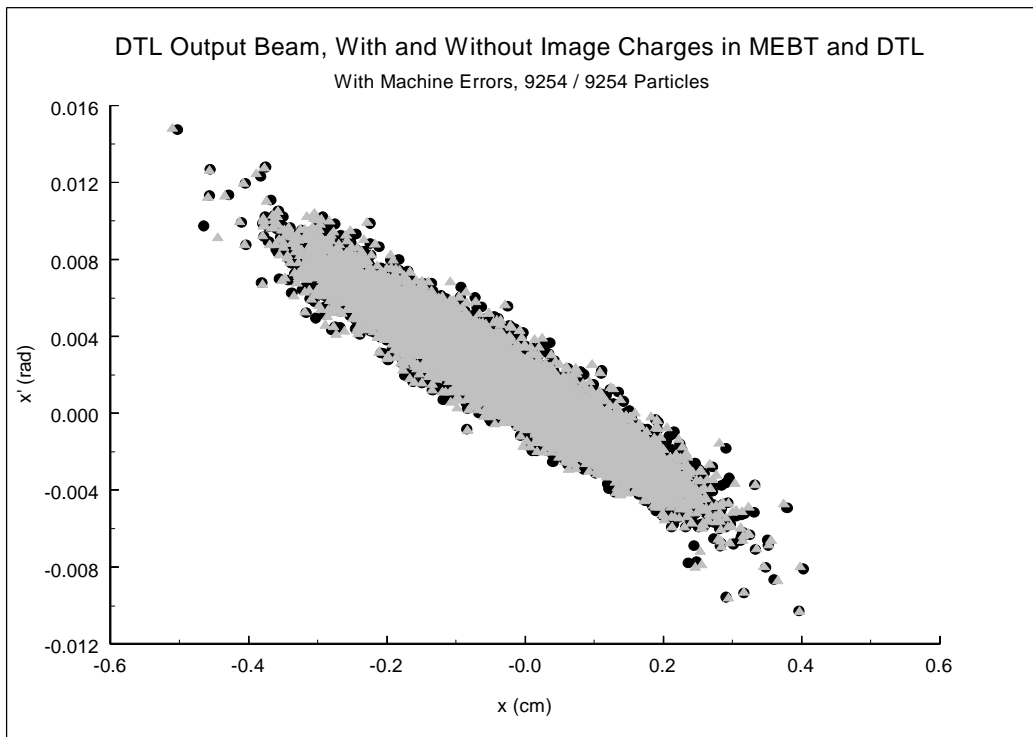


Figure 4a. Horizontal phase space of unchopped DTL output beam, machine errors, 2D space-charge routine, with and without image charges in MEBT and DTL.

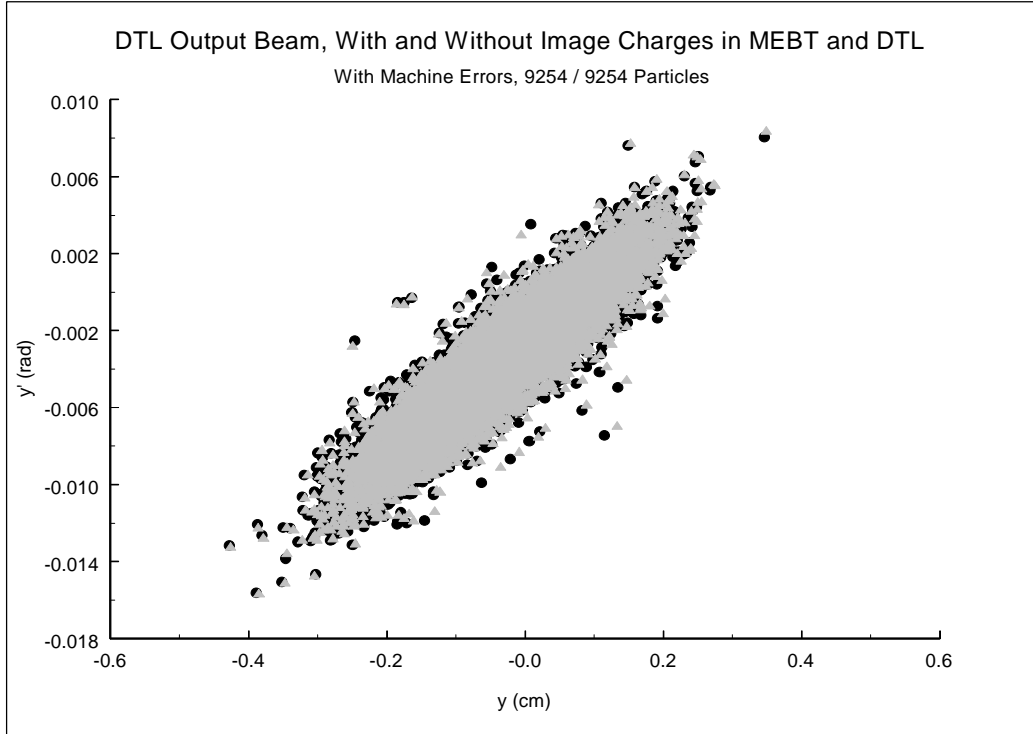


Figure 4b. Vertical phase space of unchopped DTL output beam, machine errors, 2D space-charge routine, with and without image charges in MEBT and DTL.

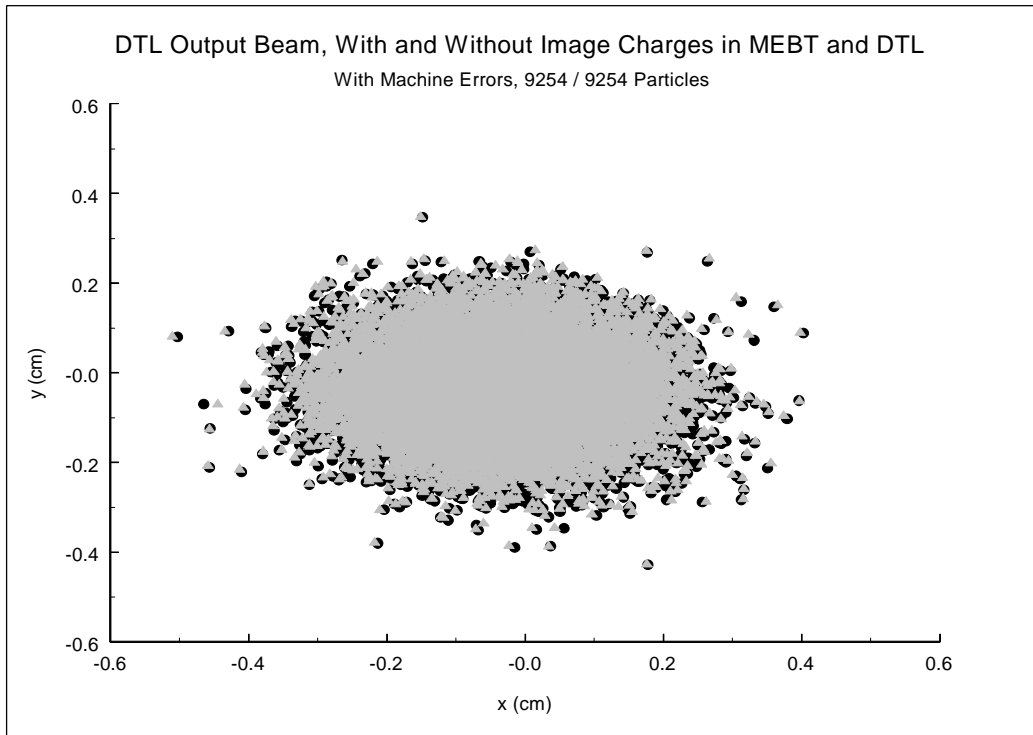


Figure 4c. Footprints of unchopped DTL output beam, machine errors, 2D space-charge routine, with and without image charges in MEBT and DTL.

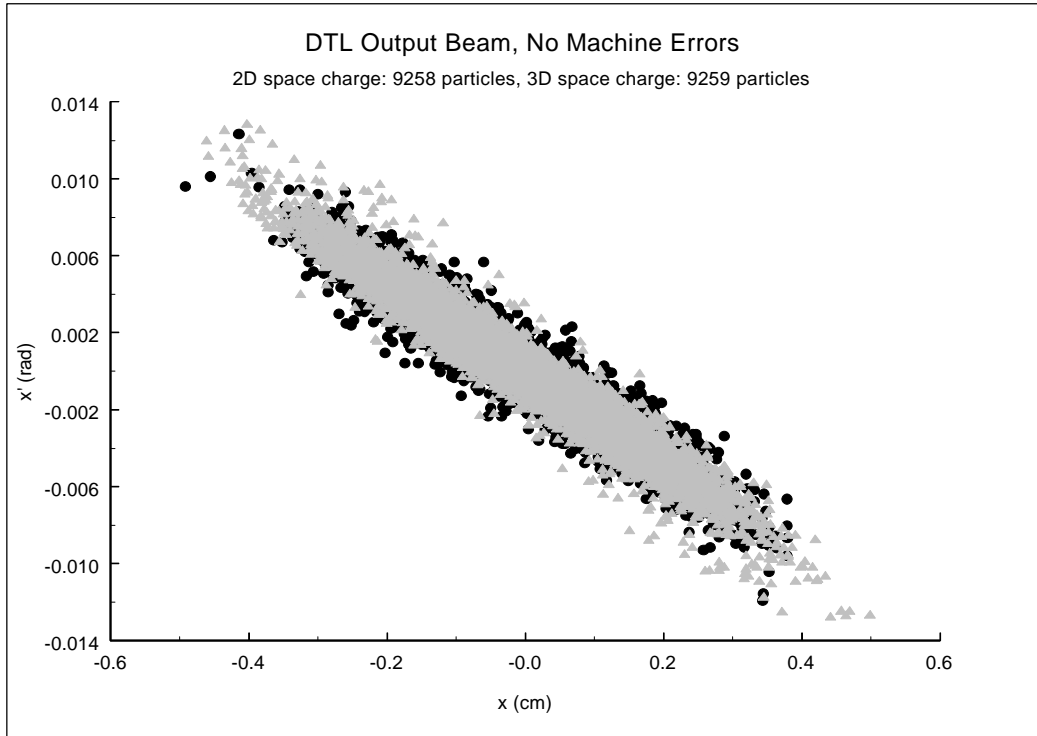


Figure 5a. Horizontal phase space of unchopped DTL output beam, no machine errors, no image charges, with 2D and with 3D space-charge routine.

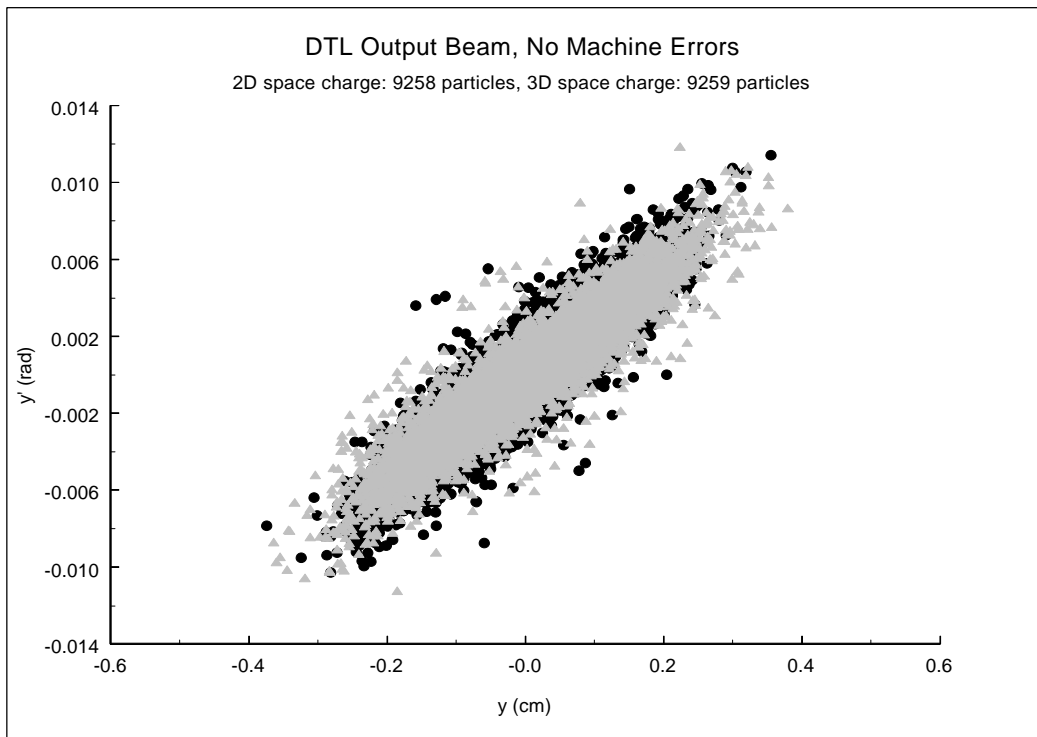


Figure 5b. Vertical phase space of unchopped DTL output beam, no machine errors, no image charges, with 2D and with 3D space-charge routine.

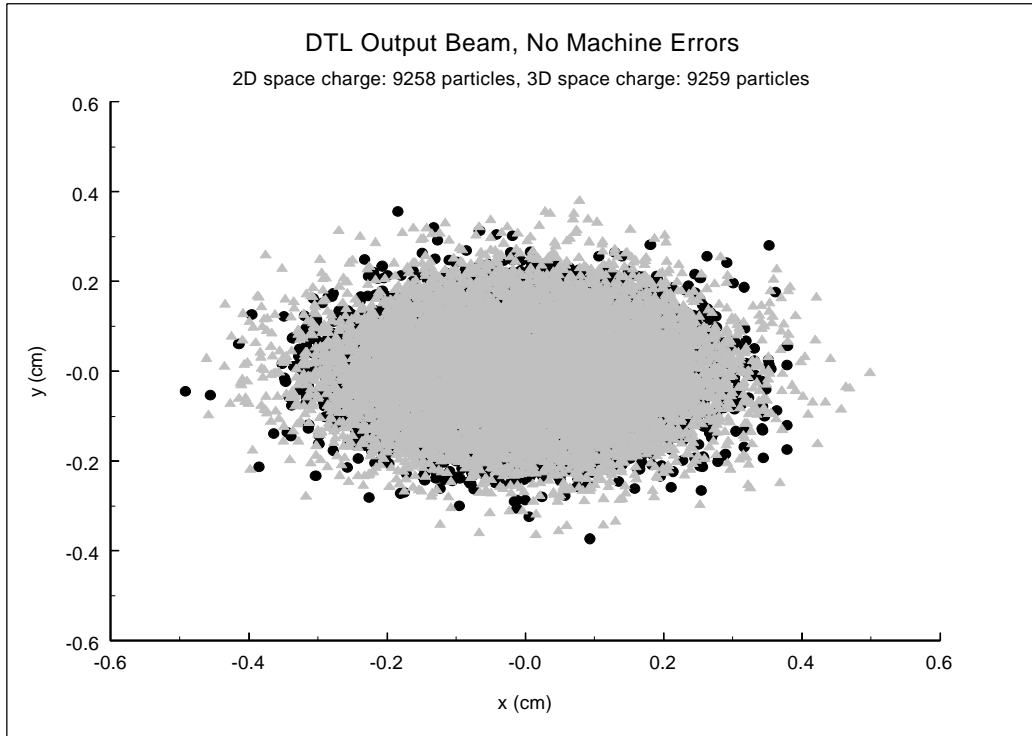


Figure 5c. Footprints of unchopped DTL output beam, no machine errors, no image charges, with 2D and with 3D space-charge routine.

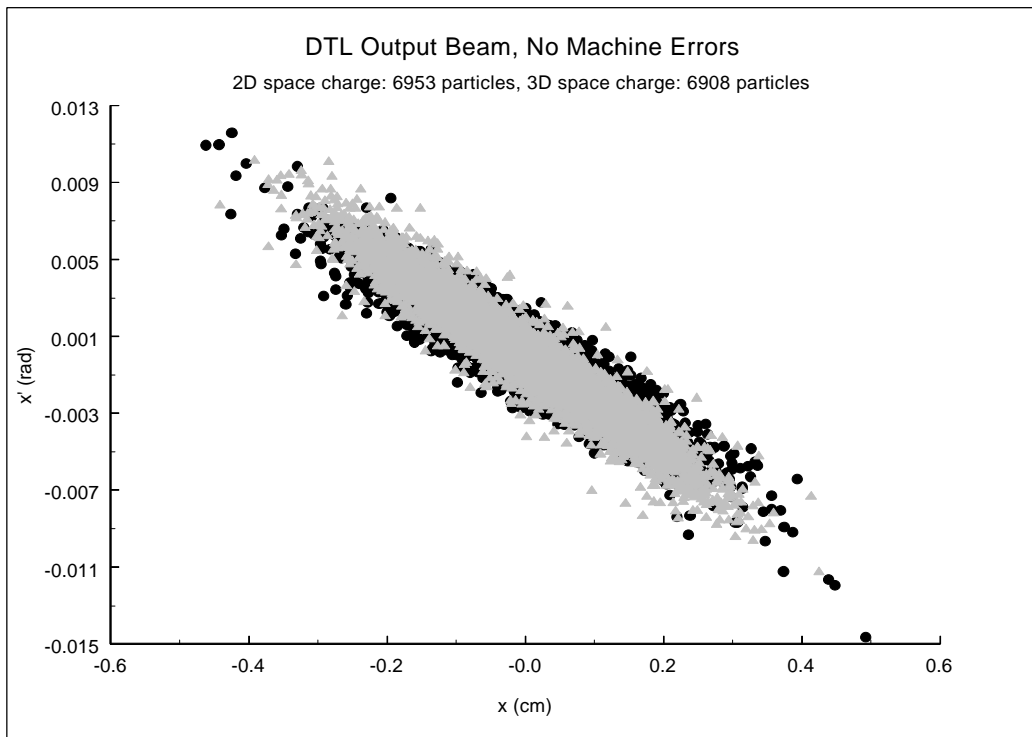


Figure 6a. Horizontal phase space of partially chopped DTL output beam, no machine errors, no image charges, with 2D and with 3D space-charge routine.

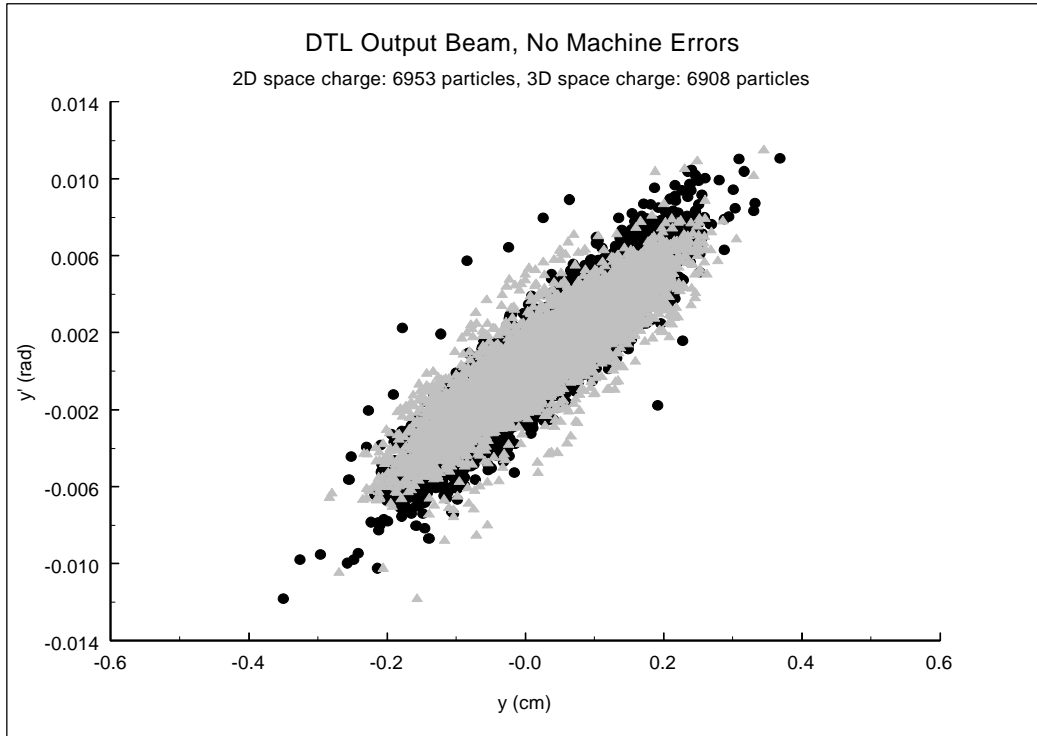


Figure 6b. Vertical phase space of partially chopped DTL output beam, no machine errors, no image charges, with 2D and with 3D space-charge routine.

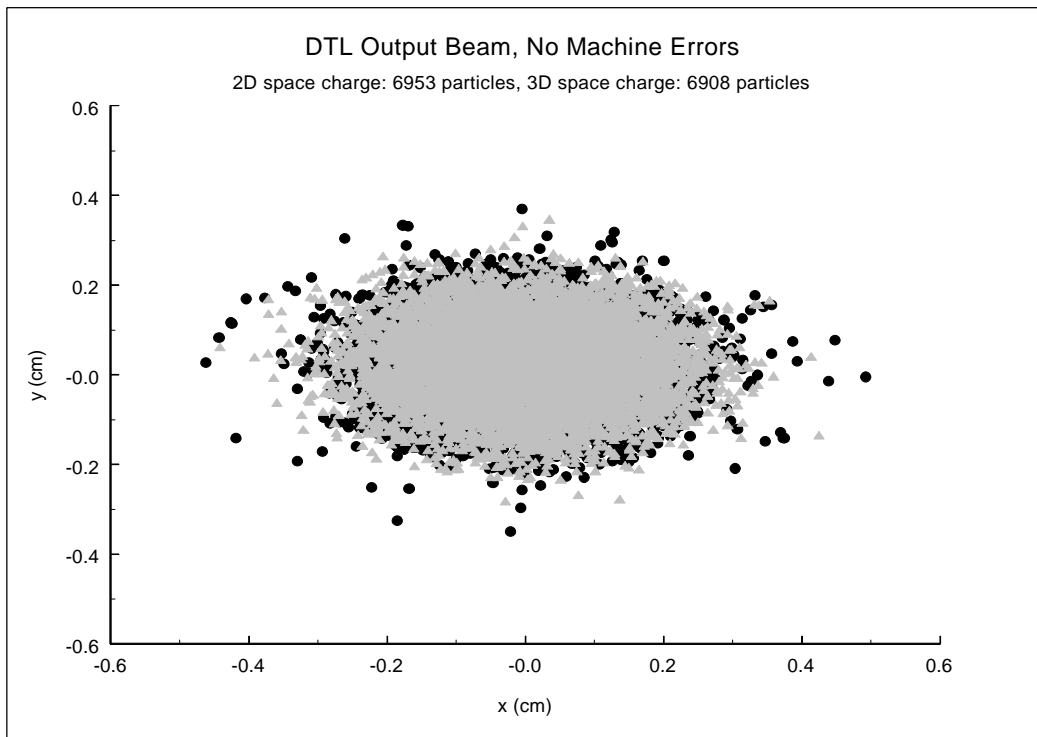


Figure 6c. Footprints of partially chopped DTL output beam, no machine errors, no image charges, with 2D and with 3D space-charge routine.

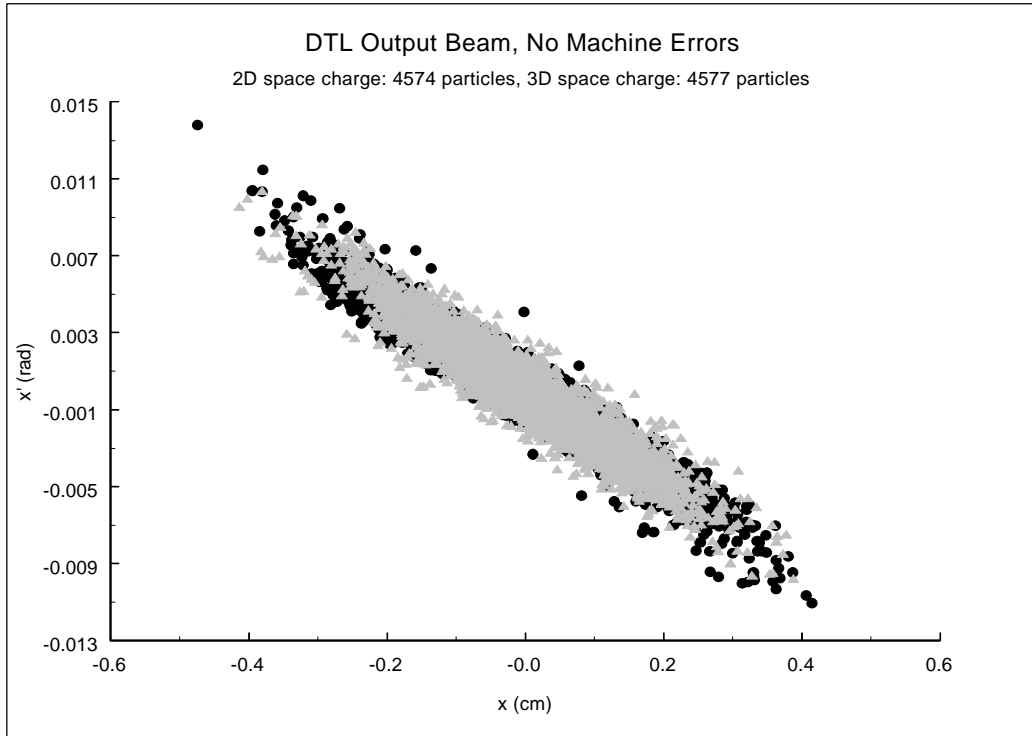


Figure 7a. Horizontal phase space of partially chopped DTL output beam, no machine errors, no image charges, with 2D and with 3D space-charge routine.

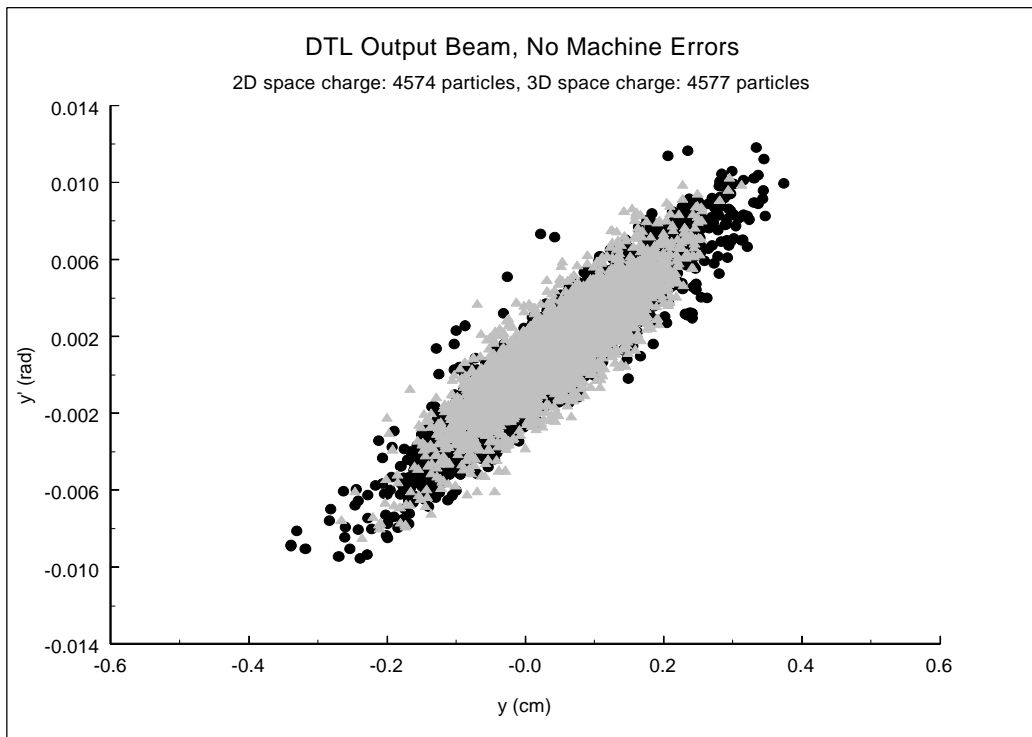


Figure 7b. Vertical phase space of partially chopped DTL output beam, no machine errors, no image charges, with 2D and with 3D space-charge routine.

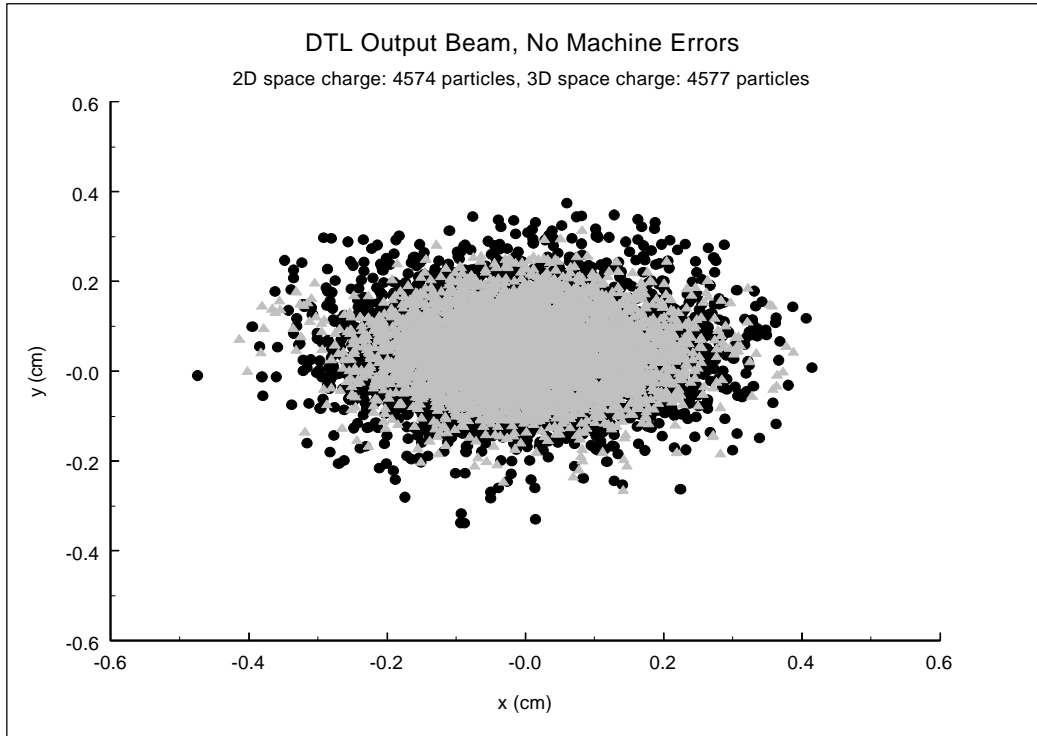


Figure 7c. Footprint of partially chopped DTL output beam, no machine errors, no image charges, with 2D and with 3D space-charge routine.

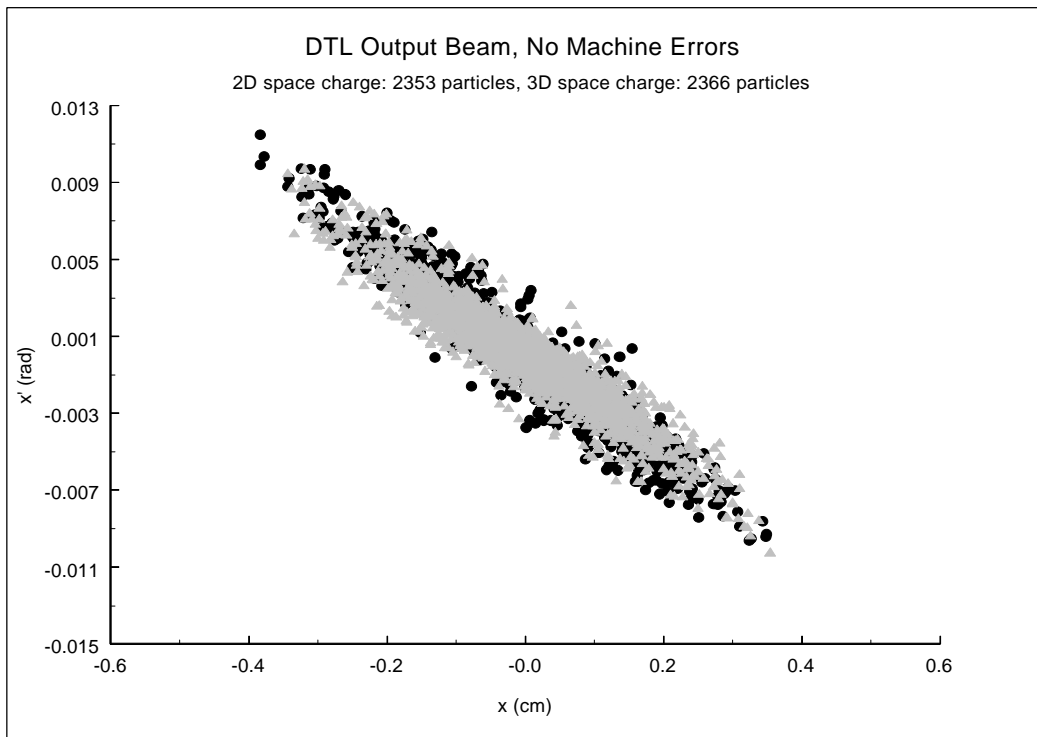


Figure 8a. Horizontal phase space of partially chopped DTL output beam, no machine errors, no image charges, with 2D and with 3D space-charge routine.

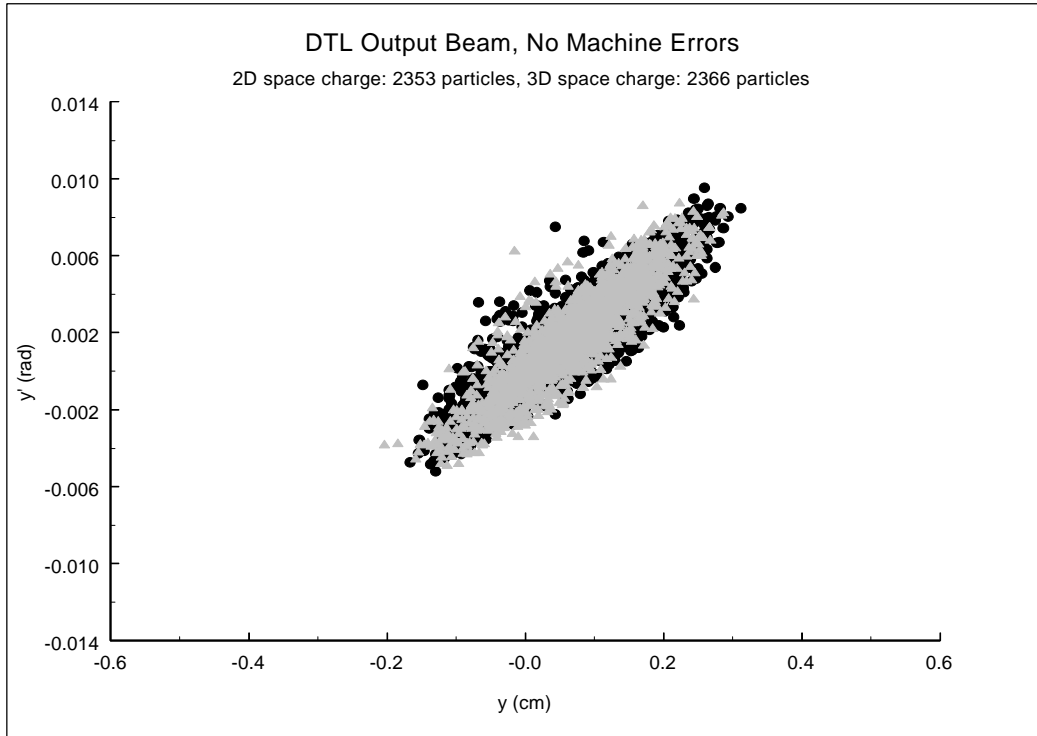


Figure 8b. Vertical phase space of partially chopped DTL output beam, no machine errors, no image charges, with 2D and with 3D space-charge routine.

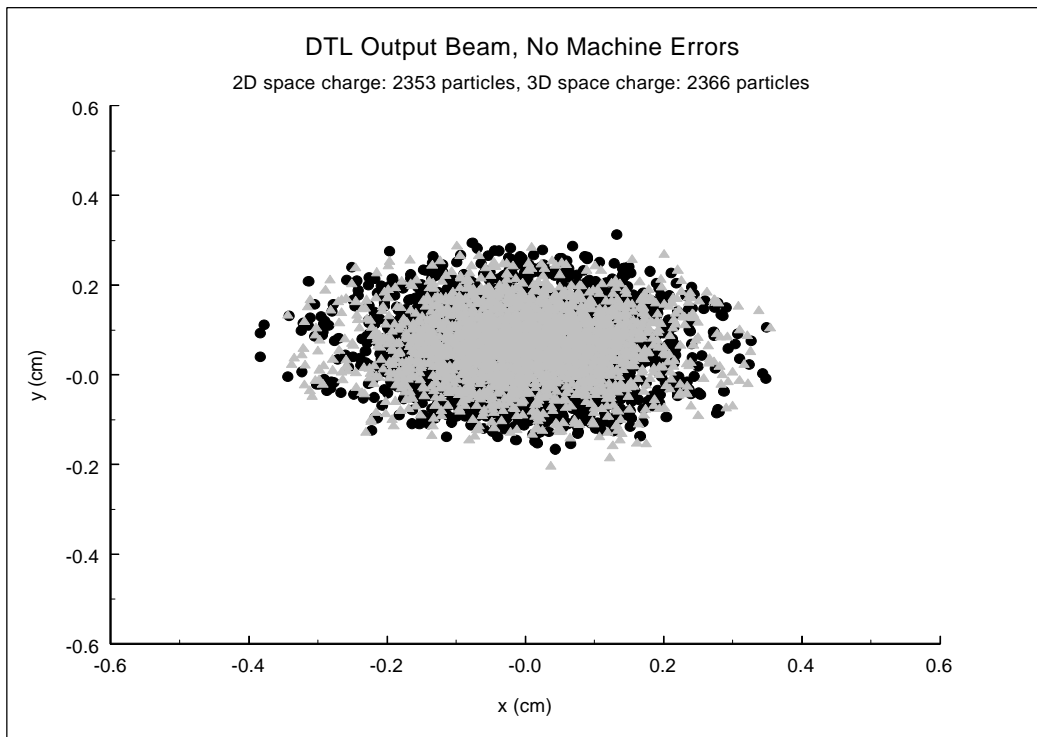


Figure 8c. Footprints of partially chopped DTL output beam, no machine errors, no image charges, with 2D and with 3D space-charge routine.

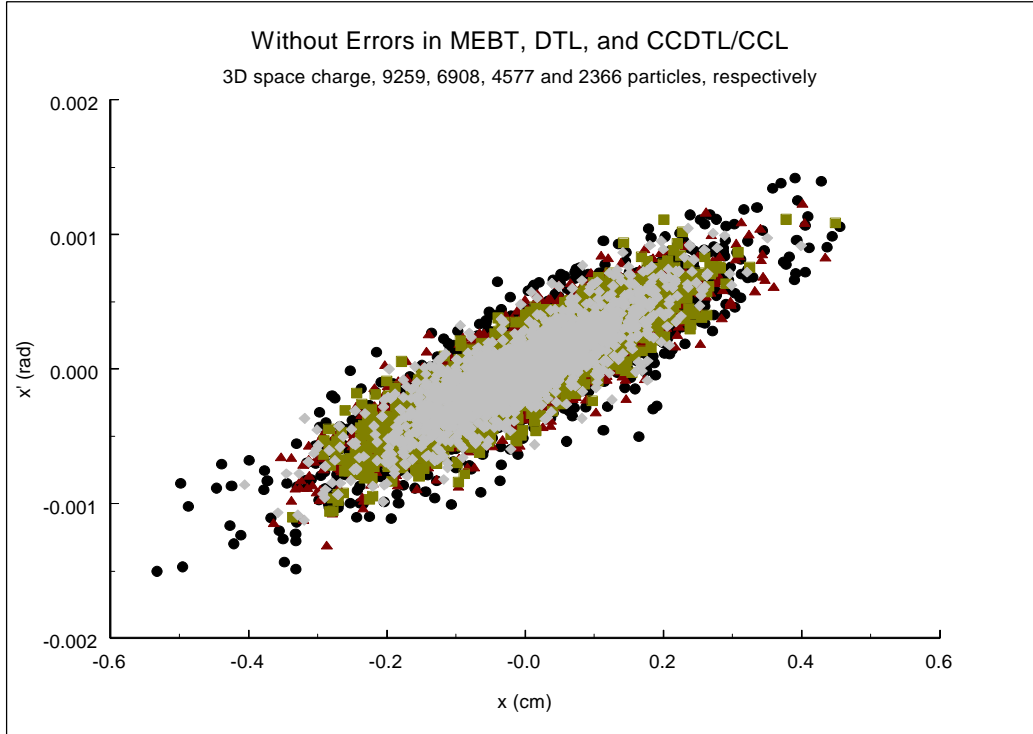


Figure 9a. Horizontal phase space of unchopped and partially chopped CCL output beams, no machine errors, no image charges, 3D space-charge routine in MEBT, DTL.

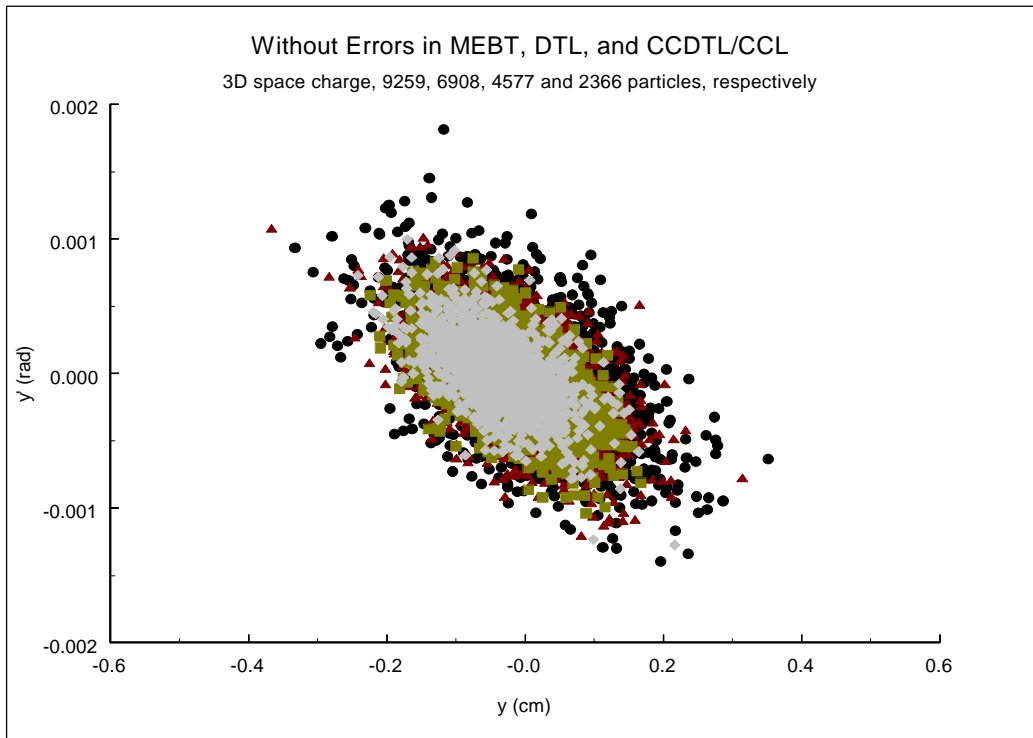


Figure 9b. Vertical phase space of unchopped and partially chopped CCL output beams, no machine errors, no image charges, 3D space-charge routine in MEBT, DTL.

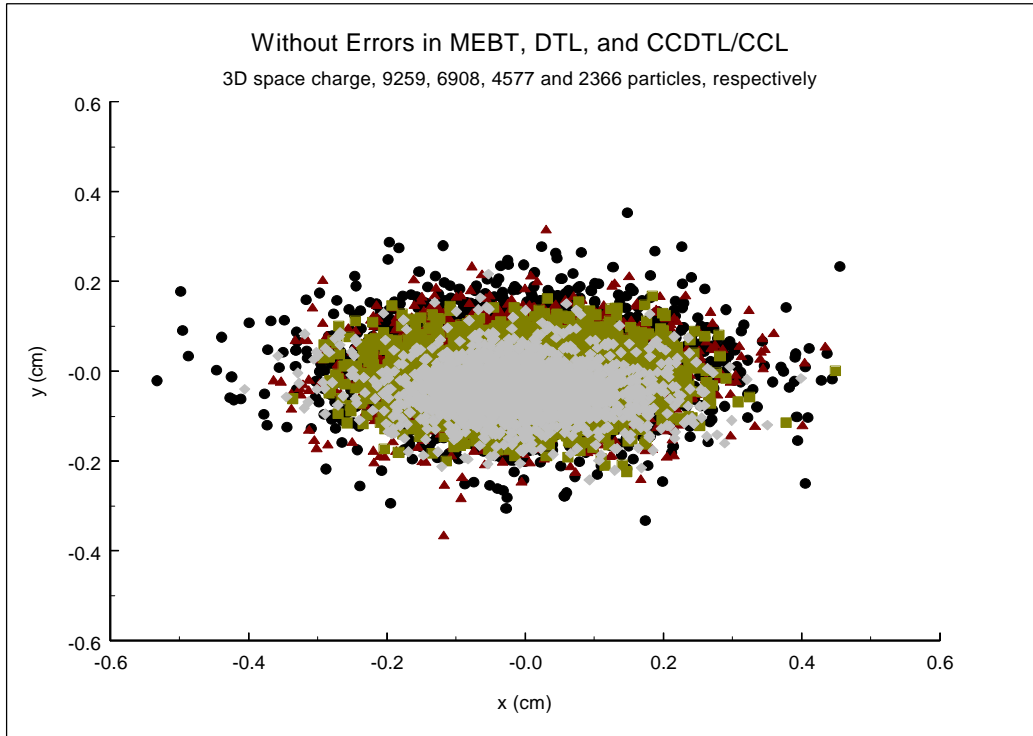


Figure 9c. Footprints of unchopped and partially chopped CCL output beams, no machine errors, no image charges, 3D space-charge routine in MEBT, DTL.

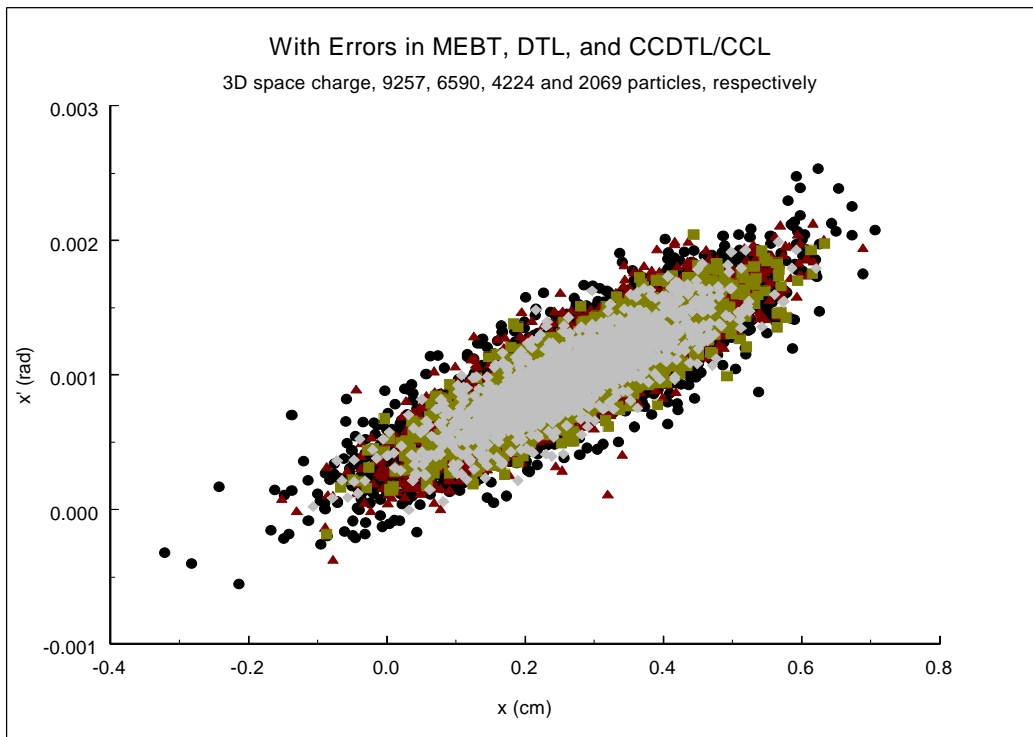


Figure 10a. Horizontal phase space of unchopped and partially chopped CCL output beams, machine errors, no image charges, 3D space-charge routine in MEBT, DTL.

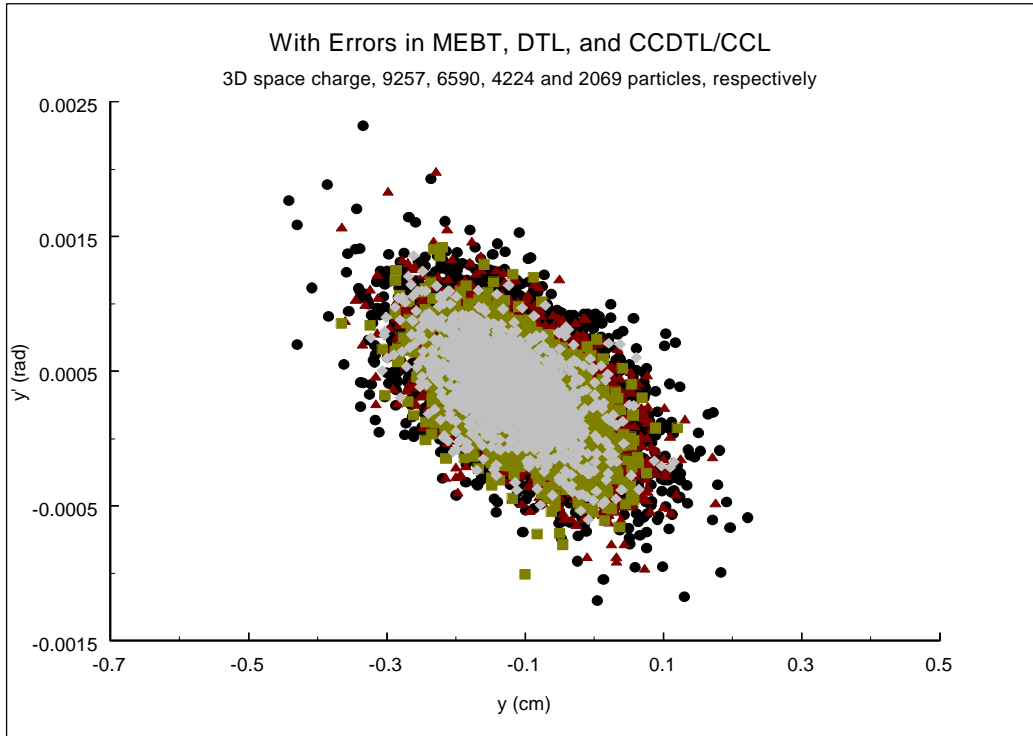


Figure 10b. Vertical phase space of unchopped and partially chopped CCL output beams, machine errors, no image charges, 3D space-charge routine in MEBT, DTL.

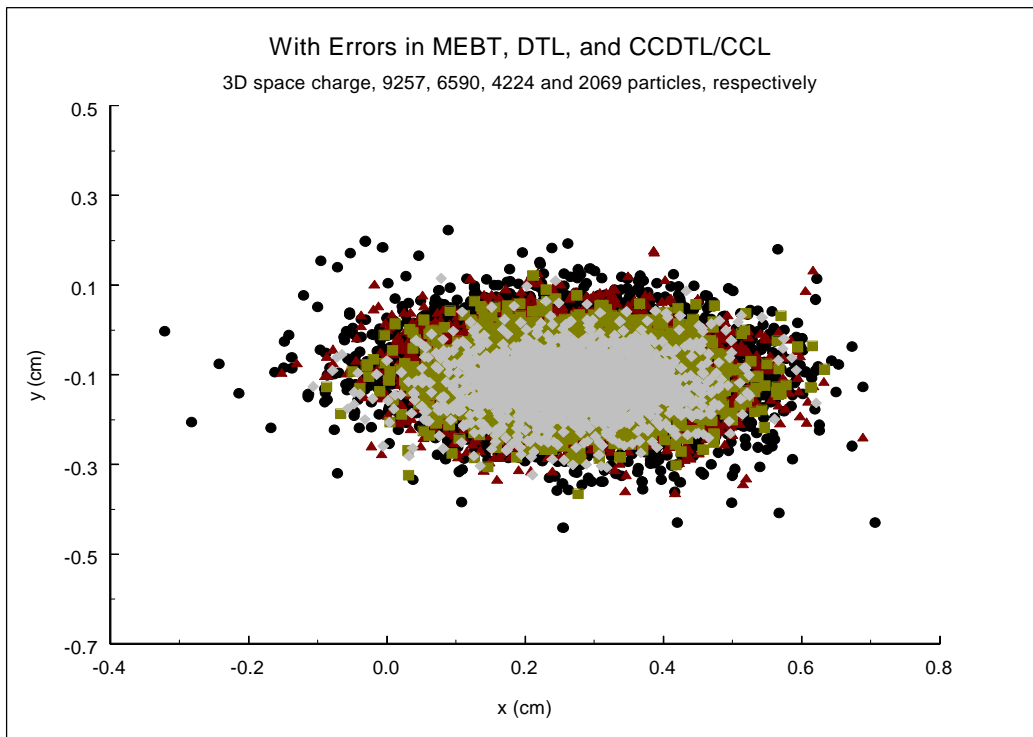


Figure 10c. Footprints of unchopped and partially chopped CCL output beams, machine errors, no image charges, 3D space-charge routine in MEBT, DTL.